Compton scattering of 320-keV γ rays by K-shell electrons of holmium and gold

Saharsha M. Lad, G. Basavaraju, and P. P. Kane
Department of Physics, Indian Institute of Technology, Powai, Bombay 400 076, India
(Received 15 January 1990; revised manuscript received 18 April 1990)

Compton scattering of 320-keV γ rays through 45° and 115° by K-shell electrons of gold and holmium has been studied by the well-known coincidence technique. Double-differential cross sections with respect to outgoing photon energy and angle have been determined from 30 keV up to the kinematic limits. Target-Z-dependent false coincidences arising from bremsstrahlung emitted by photoelectrons were estimated both by theoretical analysis and by measurements carried out with gold targets of thicknesses differing by more than a factor of 4. The analysis of the bremsstrahlung process included the often neglected effects of the angular distribution of photoelectrons and of multiple scattering of electrons during the slowing-down process within the target. The bremsstrahlung generated false coincidences obscure the possible observation of the predicted infrared divergence in the low outgoing photon energy regime and lead to a significant contribution even in the quasi-Compton regime. The single-differential cross sections obtained after a correction for bremsstrahlung are in reasonable agreement with theoretical calculations.

I. INTRODUCTION

Two recent reports[1,2] from this laboratory described in detail, experimental and theoretical results pertaining to Compton scattering of 279.2-keV γ rays by K-shell electrons of tin and gold. Double-differential cross sections with respect to angle and outgoing photon energy were also reported[3] sometime ago from another laboratory in the case of 320-keV γ rays and tin, holmium, and gold targets. In the regime of low outgoing photon energies, increasing cross sections with decreasing photon energy representing an infrared divergence (IRD) effect in scattering were measured in these experiments. Contrary to theoretical expectations[4] a larger IRD effect was reported in Ref. 3 with holmium rather than gold. Although a significant error in Ref. 3 concerning the estimate of bremsstrahlung generated false coincidences was pointed out in Ref. 1, the magnitude of the error was underestimated on account of an inadvertent omission in Ref. 1 in the method of estimation. In view of this situation, it was considered worthwhile to perform new measurements with 320-keV γ rays, and also to make a detailed analysis of the relevant bremsstrahlung problem. Many details concerning the present experiment are the same as in Refs. 1 and 2. Only specific details pertaining to the present 320-keV experiment, the results obtained, and a fresh analysis of false coincidences will be presented here. It is now clear that previous claims regarding an unambiguous observation of the infrared divergence effect were premature. Further, a significant correction will be shown to be necessary even in the quasi-Compton peak energy regime.

New results have been reported[5] recently concerning Compton scattering of 70-keV synchrotron radiation by K-shell electrons of copper. A detailed estimate of false events of secondary origin has been presented in that report. The energy spectrum in the IRD regime was shown in this case also to be dominated by bremsstrahlung generated false events.

Specific details regarding the present experiment and a transparent method for the estimation of target-Z-dependent false coincidences will be presented in Sec. II. The results will be discussed in Sec. III.

II. EXPERIMENTAL DETAILS, TARGET-Z-DEPENDENT FALSE COINCIDENCES, AND DOUBLE-DIFFERENTIAL CROSS SECTIONS

A. Experimental details

Chromium-51 sources of approximately 800 mCi initial strength were used in the present experiment. The half-life of this electron capture source is only 28 days and 320-keV γ rays are emitted in only 10% of the decays, so two similarly prepared sources were used during measurements at 45° and 115°. Note that in an early study[6] with this source, detailed double-differential distributions extending downwards to low photon energies have not been reported. The well-known procedure of detecting scattered photons in coincidence with characteristic K x rays of the target was adopted in the present experiment.

The number of net coincidences N_t with the target under study were determined by a subtraction of the chance coincidences $N_{\rm ch}^T$ and the target-Z-independent net false coincidences N_f from the total number of coincidences N^T measured with the target:

$$N_t = N^T - N_{\rm ch}^T - N_f \ . \tag{1}$$

The target-Z-independent false coincidences were obtained with the help of an aluminum target containing the same number of electrons as the target under study. To achieve at least moderate precision, coincidence counting times of about 200 h were needed for each type of measurement with each target at each angle. The different count rates are summarized in Table I.

Self-supporting targets of better than 99.9% purity

TABLE I. Integrated coincidence count rates above 100 keV per 3.6×10^3 sec. The source strengths were different for different cases. The quoted statistical errors have been obtained by collecting data of each kind for about 7.2×10^5 sec. Here N^T is the coincidence rate measured with a target under study, N_{ch}^T is the corresponding chance coincidence count rate, N_f is the target-Z-independent false count rate, and N_t is the net coincidence count rate.

Angle (deg)	Target	N^T	N_{ch}^T	N_f	$N_t=N^T-N_{ch}^T-N_f$
45	Gold	42.8±0.49	0.69±0.06	10.25±0.24	31.9±0.55
	Holmium	17.4±0.36	1.56±0.11	11.1±0.29	4.74±0.47
115	Gold	21.5±0.41	1.65±0.11	7.25±0.25	12.6±0.49
	Holmium	9.26±0.29	0.48±0.07	4.09±0.19	4.69±0.38

were used. Although most of the measurements were made with 40.5 mg/cm^2 gold and 30 mg/cm^2 holmium targets, additional measurements were also made with a 9.17 mg/cm^2 gold target with the intention of obtaining an experimental determination of bremsstrahlung generated false counts. A similar procedure was followed in several earlier studies including those reported in Refs. 2 and 3. The above-mentioned gold target thicknesses correspond, respectively, to 0.34 and 0.075 of the (240-keV) photoelectron range of 120 mg/cm^2, calculated according to the continuous showing-down approximation[7] (CSDA). The values of double-differential cross sections deduced from experiments with the thinner and the thicker gold targets were consistent with each other within the experimental error of about 20%. This result, obtained also in earlier studies, can be understood in the context of the analysis to be presented in Sec. II C. Corrections for target-Z-dependent false contributions are described in Secs. II B and II C.

B. Contributions from source backscattered photons

Photons of 320 keV after inelastic backscattering from the source material and the source housing have an energy of about 145 keV and a relative intensity of about 8% in this experiment. The energy distributions resulting from K-shell Compton scattering of these photons extend to kinematic limits of 64 and 90 keV, respectively, in the case of gold and holmium. Nonrelativistic theoretical calculations briefly described in Sec. III were used to estimate this relatively small but not totally negligible contribution to the coincidence counts in the low-energy regime. A correction of this type has not been mentioned in earlier reports.

C. Bremsstrahlung from electrons released through K-shell photoeffect

The process mentioned above leads to the detection of target K x rays in coincidence with bremsstrahlung photons and is mainly responsible for Z-dependent false counts.

The window of about 28 keV of the single-channel analyzer (SCA) at the output of the thin or the so-called x-ray detector, adjusted for the selection of K x-ray pulses, restricted also the possible energy range of the bremsstrahlung photons detected by the same counter. As pointed out in Ref. 1 the detection of K x rays by the γ counter in coincidence with bremsstrahlung photons accepted by the x-ray detector SCA window is mainly responsible for the observation of K x-rays in the γ counter spectra recorded in the coincidence gated mode. Since the positions and widths of K x-ray peaks in the γ counter spectra could be accurately determined, a straightforward procedure was used to subtract the contribution of such Z-dependent false counts from the recorded spectra.

Now we will discuss in some detail false coincidences arising on account of simultaneous detection of K x rays by the x-ray detector and bremsstrahlung photons by the γ counter.

The number of K x rays detected per unit time by the x-ray detector is obtained by a summation of contributions from different layers of the target of small thickness δt. The contribution δN_x from one such layer is given by Eq. (2):

$$\delta N_x = N_0 \delta N_{sc} \sigma_{pK} (\omega_K/4\pi) \eta_K \Omega_K a_K \epsilon_K \ , \tag{2}$$

N_0 represents the number of γ rays incident on the target per unit time, δN_{sc} represents the number of scatterer atoms per unit area in a layer of small thickness δt, σ_{pK} represents the K-shell photoeffect cross section of a target atom, ω_K represents the K-shell fluorescence yield, η_K represents the single-channel analyzer window acceptance factor for target K x rays, and Ω_K, a_K, and ϵ_K are the solid angle, the transmission, and the efficiency for the detection of K x rays, respectively. Corresponding to each K x-ray detection, the probability P_{Kb} of simultaneous detection of bremsstrahlung photons of energy k_f by the γ counter is given by Eq. (3):

$$P_{Kb} = \int \frac{d^2\sigma_b}{d\Omega dk_f} dN_{sc} \Omega \epsilon_{k_f} a_{k_f} \ , \tag{3}$$

where $d^2\sigma_b/d\Omega dk_f$ is the atomic bremsstrahlung cross section per unit solid angle per unit energy range and is a function depending on E, k_f, ϕ, and Z, E is the electron kinetic energy, ϕ is the angle of photon emission with respect to the direction of the slowing-down electron, Z is the atomic number of the scatterer, dN_{sc} indicates the number of atoms per unit area in a further thin layer of the target traversed by the electron, the integration is over the entire electron path within the target, and Ω, a_{k_f} and ϵ_{k_f} are, respectively, the solid angle, the transmission, and the efficiency for the detection of photons of energy k_f by the γ counter. Therefore the rate $(\Delta N_b)_{\delta t}/\Delta k_f$ of Z-dependent false coincidences due to

bremsstrahlung per unit energy range is obtained from the product of δN_x and P_{Kb}:

$$\frac{(\Delta N_b)_{\delta t}}{\Delta k_f} = \left[N_0 \delta N_{\rm sc} \frac{\omega_K}{4\pi} \eta_K \Omega_K a_K \epsilon_K \Omega a_{k_f} \epsilon_{k_f} \right] \times \left[\sigma_{pK} \int \frac{d^2\sigma_b}{d\Omega dk_f} dN_{\rm sc} \right] . \quad (4)$$

Note the dependence on $(\delta N_{\rm sc})$ as well as on an integral over the number of atoms encountered in the slowing down of the electron within the target.

The rate of net coincidence counts $(\Delta N_t)_{\delta t}/\Delta k_f$ per unit energy interval arising from K-shell Compton scattering within the layer of thickness δt is similarly given by Eq. (5), which is substantially similar in form to Eq. (4):

$$\frac{(\Delta N_t)_{\delta t}}{\Delta k_f} = \left[N_0 \delta N_{\rm sc} \frac{\omega_K}{4\pi} \eta_K \Omega_K a_K \epsilon_K \Omega a_{k_f} \epsilon_{k_f} \right] \left[\frac{d^2\sigma_K}{d\Omega dk_f} \right], \quad (5)$$

where $d^2\sigma_K/d\Omega dk_f$ is the double-differential cross section for K-shell Compton scattering. The factors within the first brackets of Eqs. (4) and (5) are common so that $(\Delta N_b)_{\delta t}/\Delta k_f$ is proportional to

$$\left[\sigma_{pK} \int \frac{d^2\sigma_b}{d\Omega dk_f} dN_{\rm sc} \right]$$

and $(\Delta N_t)_{\delta t}/\Delta k_f$ is proportional to $d^2\sigma_K/d\Omega dk_f$. The same proportionalities will apply for the respective contributions from the whole target. In the following discussion, the factor

$$\left[\sigma_{pK} \int \frac{d^2\sigma_b}{d\Omega dk_f} dN_{\rm sc} \right]$$

will be called the "apparent" bremsstrahlung cross section, which is seen to be target thickness dependent as long as the target thickness is smaller than the electron range.

The omission mentioned in the Introduction in connection with similar estimates reported in Refs. 1 and 2 is traceable to an inadvertent neglect of the solid angle Ω in Eq. (5). The omission resulted in an underestimate of the ratio $(\Delta N_b)/\Delta N_t$ by a factor $1/\Omega$, i.e., by a factor of about 50. Thus the relative importance of bremsstrahlung was erroneously underestimated.

To estimate the apparent bremsstrahlung cross section, the target was divided into a large number (~ 15) of layers of small thickness. Electron emissions in different directions with respect to the incident photon direction were weighted with appropriate relative probabilities calculated from the results of Ref. 8. The details of the calculation are similar to those in Ref. 5, which, however, assumed isotropic emission of photoelectrons. The weighted path lengths of photoelectrons in the thicker and thinner gold targets turned out to be about 53 and 19 mg/cm^2, respectively. In the first instance, values of $d^2\sigma_b/d\Omega dk_f$ were obtained under the assumption of isotropic bremsstrahlung from the angle integrated cross sections tabulated by Pratt *et al.*[9] with the use of a scaling factor $\beta^2 k_f/Z^2$, where β is the ratio of electron velocity to velocity of light.

In contradiction to expectations based on the above estimates or on the similar estimates of Ref. 5, a variation of the "apparent" bremsstrahlung cross section with target thickness was not measurable within the experimental error of about 20% for $0.075 < t/D < 0.34$, where t/D is the ratio of the normal target thickness t to CSDA range D. The track length of electrons is much larger than the straight line path length due to multiple Coulomb scattering. In the estimation of apparent bremsstrahlung cross section, the increase in the effective track length of electrons must be taken into account in the last term in Eq. (4).

For this purpose, we will consider a recently proposed simple model.[10] According to the recent model, electrons of initial energy E_0 may be considered to move approximately in straight line paths down to a characteristic energy E_c and then below E_c to undergo random motion in the target. With this simple model, good agreement was obtained between experimental and calculated practical ranges for electrons and positrons of energy between 0.25 and 5 MeV. The practical range corresponds to electron or positron slowing down from E_0 to E_c. The results obtained according to this simple model are in agreement with trends deduced earlier[11] through Monte Carlo calculations for electrons of 0.4–4 MeV traversing normally in carbon, aluminum, and copper targets. The practical range of 250-keV electrons in gold turns out to be only 26 mg/cm^2. Thus even our thinner gold target thickness was equivalent to about 0.75 times the thickness needed to reach the condition of random motion. Consequently, the effective track length for electrons in the thinner gold target will be only about 25% less than that in the thicker gold target. Thus the above-mentioned experimental inability to measure thickness variation of the apparent bremsstrahlung cross section can be understood.

The semiempirical thick target bremsstrahlung formula,[12] developed a long time ago, is therefore useful in the interpretation of the experimental results for the thicker gold and the holmium targets. This formula is expressed through Eq. (6):

$$\int \frac{d^2\sigma_b}{d\Omega dk_f} dN_{\rm sc} = \frac{2k'Z}{4\pi} \left[\frac{E_0 - k_f}{k_f} \right], \quad (6)$$

where the initial photoelectron kinetic energy E_0 is in this experiment equal to 240 keV in the case of gold and 265 keV in the case of holmium, k' is independent of Z and is also independent of angle under the assumption of isotropic bremsstrahlung. According to Buechner *et al.*[13] for somewhat higher electron energies, k' is about 0.4×10^{-6}/keV and may even display a residual angular dependence in spite of the tendency towards isotropy due to multiple Coulomb scattering. According to Ref. 14, k' may be approximately taken to be $(0.7\pm0.2)\times10^{-6}$/keV. We adopted the reasonable criterion that k' must not be so large as to lead to an apparent bremsstrahlung cross section larger than that measured with any target. Thus we estimated the values of k' to be 0.4×10^{-6}/keV and

0.55×10^{-6}/keV for the 115° and 45° measurements, respectively. We mention in passing that, in their low photon energy experiment with copper at 70°, Marchetti and Franck[5] used a k' value of 1.38×10^{-6}/keV.

D. Experimental determination of double-differential cross sections

The differential cross section for Compton scattering of 320-keV γ rays by an atom of a low-Z target such as aluminum is taken to be the product of Z and the well-known Klein-Nishina expression for scattering by an initially free and stationary electron. Therefore the number of counts N_s per unit time in the Compton peak, determined in the singles mode with an aluminum target, is proportional to the product of the number of incident γ rays N_0, the γ detector solid angle Ω, the number of aluminum atoms per unit area, and the Klein-Nishina expression, the constant of proportionality depending on the aluminum target transmission and the γ detector efficiency. Thus with the help of the ratio of $(\Delta N_t/\Delta k_f)$ to N_s, the factors N_0 and Ω are eliminated and the double-differential cross sections for an atom of a high-Z target are expressed in terms of the Klein-Nishina cross section. This procedure has been described in greater detail in Sec. II B of Ref. 2. The calculated "apparent" bremsstrahlung cross sections and the measured values of K-shell cross sections uncorrected for bremsstrahlung are shown in Figs. 1 and 2 for gold at 115° and holmium at 45°. The similar data for gold at 45° and for holmium at 115° are not shown. As already mentioned in the beginning of Sec. II C, K x-ray peaks are not shown in these and subsequent figures. On the contrary, the presentations in Refs. 1, 2, and 3 include the K x-ray peaks.

III. DISCUSSION OF RESULTS

A. Double-differential cross sections

A subtraction of the apparent bremsstrahlung contributions from the experimental cross sections leads to double-differential cross sections, $d^2\sigma_K/d\Omega dk_f$, for K-shell Compton scattering. Below about 120 keV, the subtraction results in relatively large errors in the differences which are therefore not exhibited separately. The differences above selected energy thresholds are shown in Figs. 3–5. The double-differential scattering cross sections for gold at 45° are not shown because the measurements for this case, studied near the end of the useful life of the chromium-51 source, have poorer precision.

In order to obtain theoretical estimates, the nonrelativistic form-factor amplitude, evaluated by Schnaidt[15] and representing the contribution of the the A^2-dependent interaction term, was constructively added to the amplitude arising from the $\mathbf{A}\cdot\mathbf{p}$ interaction. Here, $\mathbf{A}$ and $\mathbf{p}$ represent the vector potential of the electromagnetic radiation and the electron momentum operator, respectively. This combination of amplitudes is indicated by the work of Bannett *et al.*[16] and has also been described in more detail in Sec. III of Ref. 2. The $\mathbf{A}\cdot\mathbf{p}$ contribution was evaluated in terms of generalized hypergeometric functions by Gavrila, who also provided a tabulation of values calculated in the dipole approximation. The amplitude arising from the constructive addition of the Gavrila and the form-factor contributions was squared to give the nonrelativistic predictions, labeled GFF, for the double-differential cross sections. The importance of properly taking both amplitudes into account is evident from Fig. 6, where the separate cross sections

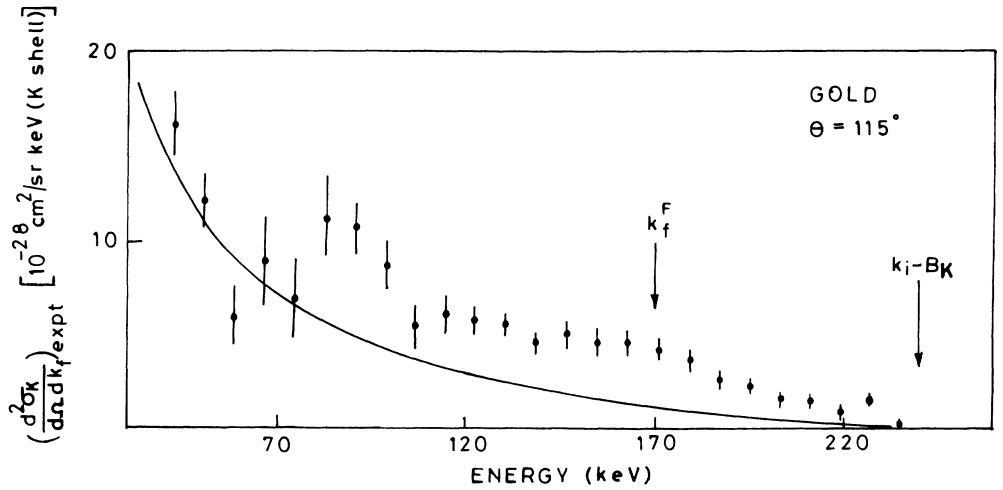

FIG. 1. Experimental results including the bremsstrahlung contribution in the case of gold at 115° scattering angle for double-differential cross sections per unit solid angle per keV per K shell. The solid curve shows theoretical estimates of the "apparent" bremsstrahlung cross section (see Sec. II C). k_f^F indicates the calculated energy of photons after Compton scattering by electrons initially free and at rest. $k_i - B_K$ is the kinematic limit of photon energy after Compton scattering by K-shell electrons. k_i is the incident photon energy and B_K is the K-shell binding energy.

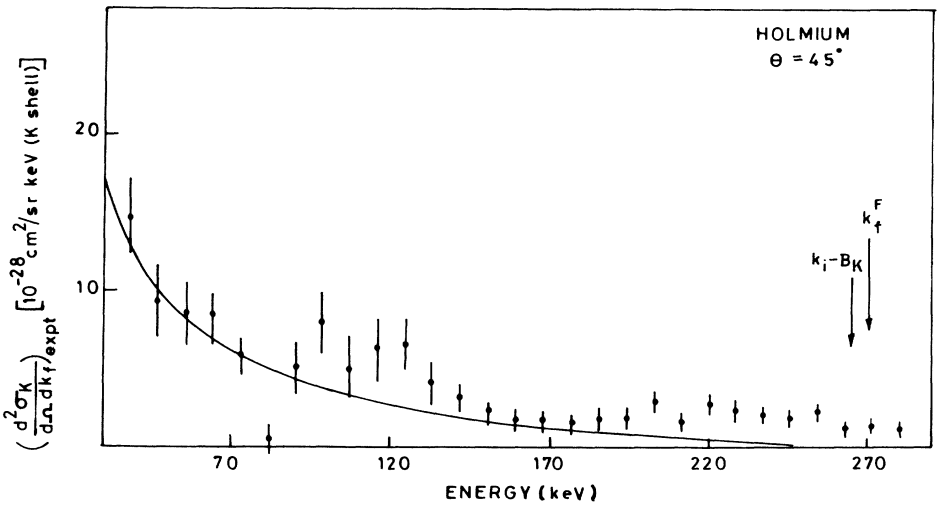

FIG. 2. The same details as for Fig. 1 except that the target is holmium and the angle of scattering is 45°.

FF and G arising from the form factor and the Gavrila calculations, and the cross sections GFF are shown in the case of gold at 115°. In the low-energy region, the GFF cross sections for gold are consistent with the differences deducible from Fig. 1 within their large errors. A similar situation has been noted by us in the other cases reported here. However, firm conclusions cannot be stated regarding an unambiguous observation of the predicted infrared divergence.

The unpublished relativistic calculations of Wittwer[17] for gold at 120° are also shown in Fig. 3. These calculations are not available for holmium and are available for gold only at 30° intervals between 0° and 180°. Note also that these calculations were made with the neglect of bound intermediate states and with the inclusion of only dipole and quadrupole contributions in a multipole expansion of the transition amplitude. Since $(1/\hbar c)(\mathbf{k}_i - \mathbf{k}_f)\cdot\mathbf{r}$ is of the order of unity for K-shell scattering of 320-keV γ rays, additional terms need to be calculated. The relativistic S-matrix results of Whittingham[18] for 279 keV should be more accurate but are not appropriate in the interpretation of our experiment with 320-keV γ rays.

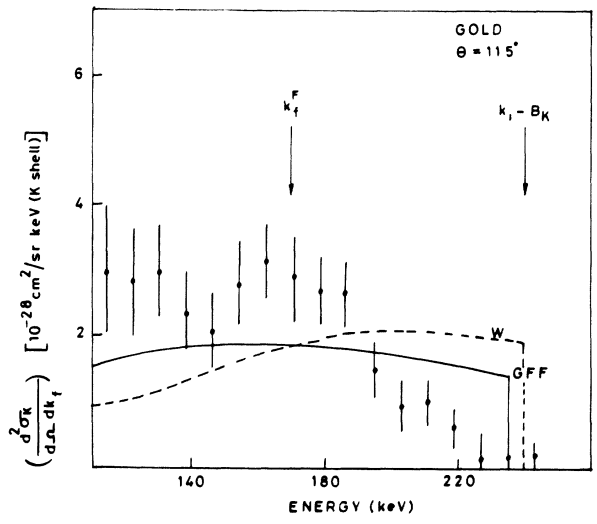

FIG. 3. The double-differential cross sections for K-shell scattering in the case of gold at 115°, deduced after a correction for the bremsstrahlung contribution. The nonrelativistic theoretical calculations at 115° labeled GFF, and relativistic calculations of Wittwer at 120°, labeled W, are also shown. The nonrelativisitic values GFF have been obtained by squaring the coherent sum of the Gavrila and the form-factor amplitudes (see Sec. III).

From Fig. 3, the scattering cross-section values for gold up to about 190 keV at 115° are larger than the theoretical nonrelativistic and relativistic calculations, the "free" Compton energy k_f^F being about 170 keV. Note that the relativistic values are larger (smaller) than the nonrelativistic values in the energy region above (below) about 180 keV. The experimental values for holmium at 115° and 45° (Figs. 4 and 5, respectively) are in reasonable agreement with the available nonrelativistic calculations. Since the kinematic limits of 240 and 265 keV for gold and holmium, respectively, are substantially larger than the "free" Compton energy at 115° but somewhat smaller than that at 45°, the broad quasi-Compton peaks are fully developed only for the 115° case, the corresponding defects toward lower energies being less than the experimental error of about 20 keV. Since the higher-energy part of the quasi-Compton peak for 45° measurements is eroded by the energy conservation requirement, an apparent defect in this case is deceptive. The nonvanishing experimental values in Fig. 5 at energies above the kinematic limit can be understood on the basis of the detector full width at half maximum of 32 keV near 270 keV.

Without the bremsstrahlung correction, the measured cross sections would have been in substantial disagreement with theory. Further, unless the measurements had been extended to low enough outgoing photon energies, it

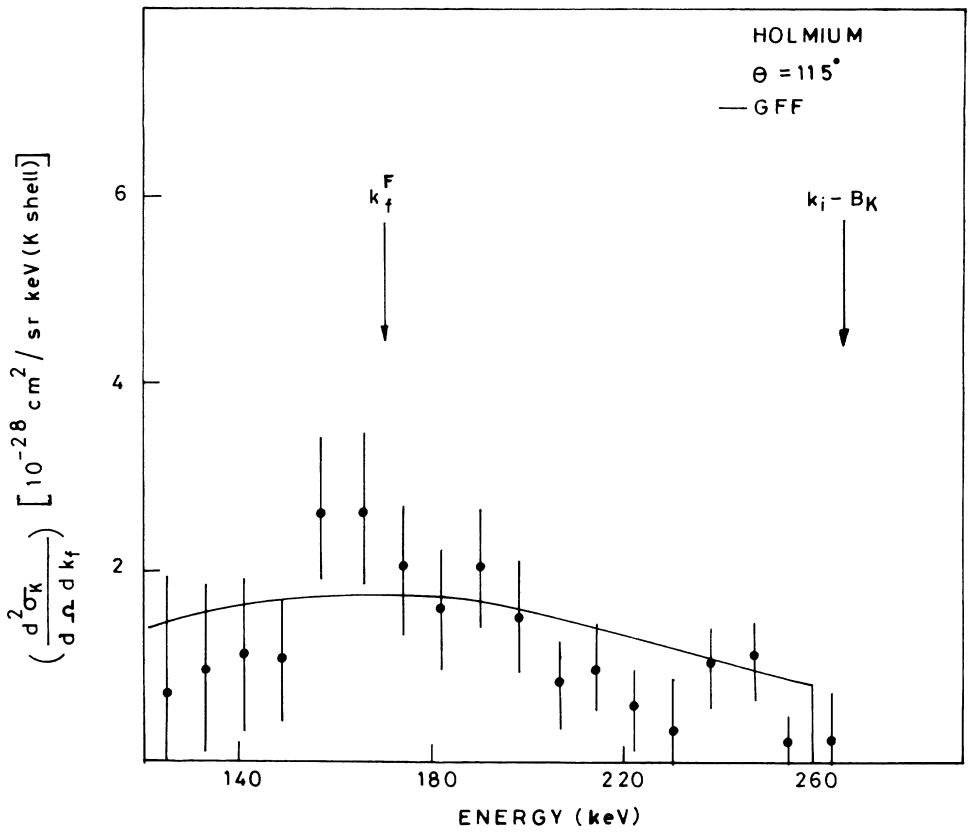

FIG. 4. The same details as for Fig. 3 except that the target is holmium and that only the nonrelativistic theoretical calculations at 115° (GFF) are shown. Relativistic calculations are not available in the case of holmium.

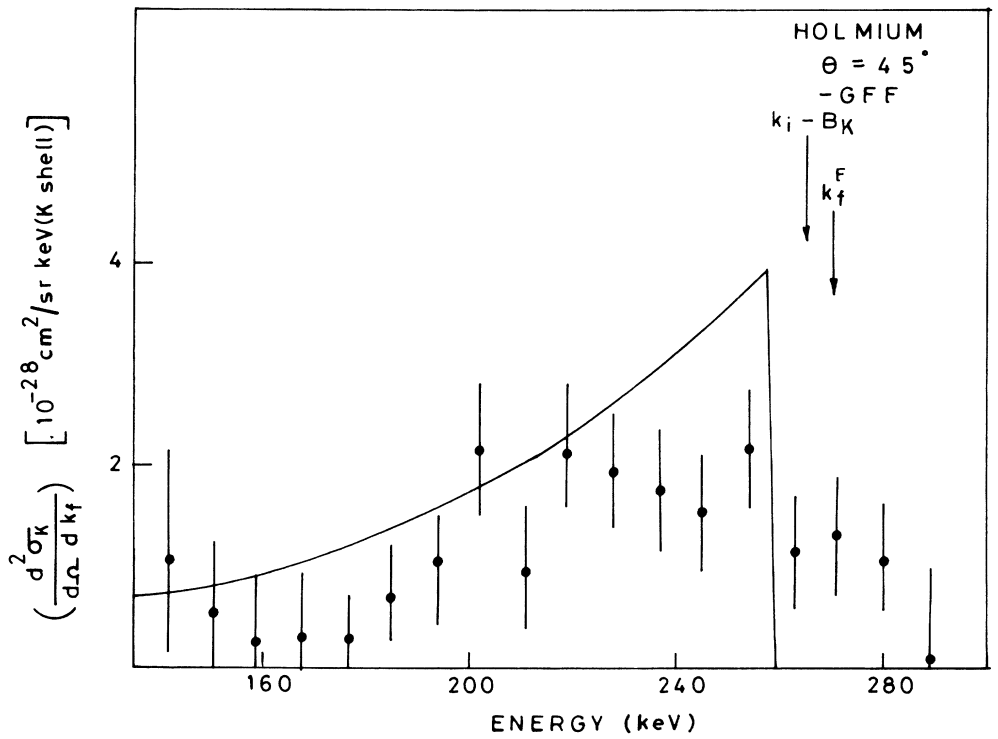

FIG. 5. The same details as for Fig. 4 except that the angle of scattering is 45°.

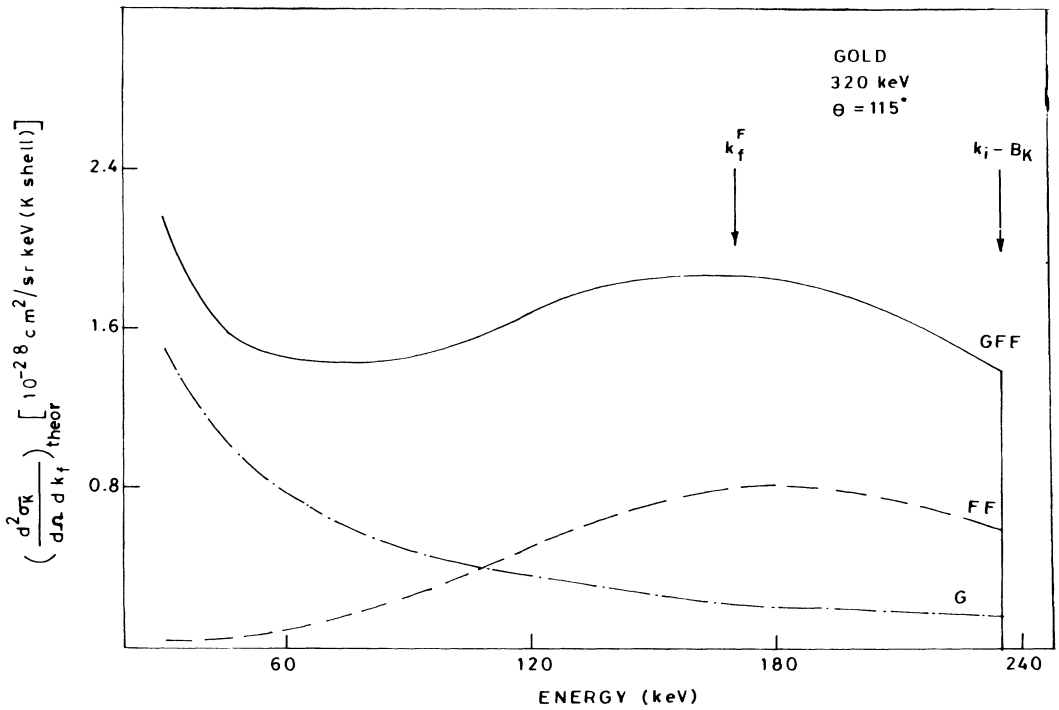

FIG. 6. Nonrelativistic theoretical values of double-differential cross sections for K-shell Compton scattering vs photon energy in the case of gold at 115°. The curve G indicates the energy distribution according to Gavrila's calculations. The curve FF indicates the energy distribution according to Schnaidt's form-factor calculations. The curve GFF represents the energy distribution calculated by squaring the coherent sum of the Gavrila and the form-factor amplitudes.

TABLE II. Cross-section ratios obtained with 320-keV γ rays in the present study and previous work. The lower-energy thresholds were 120 and 140 keV at scattering angles of 115° and 45°, respectively. The results of earlier experiments and theoretical calculations at 320 keV are also listed. The errors associated with values in the fifth column are of the order of ±0.1. The errors quoted in the fourth column are associated with reading off values from graphical presentations of Spitale and Bloom. The errors in the relativistic results given in the last column are 10–15% according to Wittwer. The Klein-Nishina cross sections per electron are 4.33×10^{-26} cm^2/sr and 1.77×10^{-26} cm^2/sr at 45° and 115°, respectively.

		Experiment			Theory	
Scattering angle	Element	Present work	Ref. 3	Ref. 6	Nonrelativistic[a]	Relativistic[b]
30°	Gold				0.13	0.11
45°	Lead			0.50		
	Gold	0.14±0.04	0.05±0.03		0.21	
	Tantalum			0.53		
	Holmium	0.21±0.03	0.13±0.02		0.25	
	Samarium			0.65		
60°	Gold		0.11±0.03		0.29	0.24
	Holmium		0.23±0.02			
110°	Lead			0.84		
	Tantalum			0.85		
	Samarium			0.91		
115°	Gold	0.69±0.06			0.56	
	Holmium	0.51±0.065			0.57	
120°	Gold		0.40±0.06			0.59
	Holmium		0.90±0.07			

[a]Nonrelativistic GFF calculations (see Sec. III A).
[b]Relativistic calculations of Ref. 17 for gold.

would not have been possible to estimate the bremsstrahlung correction. Contrary to previously made assumptions, the earlier results obtained with 279- and 320-keV γ rays are also subject to similar corrections. The higher-energy experiments with 662- and 1112-keV γ rays, references to these experiments having been cited in Ref. 2, are likely to be much less affected by this correction, since in these cases typical target thicknesses were less than 0.02 of the corresponding electron ranges.

B. Cross-section ratio

The double-differential cross sections are integrated from a selected low-energy threshold up to the kinematic limit in order to obtain the single-differential cross section, the ratio of which to the Klein-Nishina cross section for two electrons gives the K-shell cross-section ratio. The latter indicates the gross effect of electron binding on the cross section.

Table II lists the cross-section ratios obtained in the present and earlier studies as well as those calculated theoretically. The relativistic calculation is not available at 45°, so the relativistic cross-section ratios at 30° and 60° are shown in the table. From the trend of variation of cross-section ratio with angle, the relativistic value of the ratio for gold at 45° is expected to be at most 20% smaller than the tabulated nonrelativistic value. At 45°, the experimental values of Ref. 6 are much larger than all the other listed values, probably on account of inadequate attention to bremsstrahlung corrections in this early work. A similar remark also applies to the listed values in the neighborhood of 115°.

The present experimental values are in reasonable agreement with the nonrelativistic and the available relativistic calculations, the differences between the two calculations being not larger than 20% at the photon energy of about $0.6mc^2$ of this experiment. The experimental value for holmium at 120° obtained by Spitale and Bloom is surprisingly large. Note that their value for tin (not tabulated) is smaller than that for holmium, revealing an oscillatory variation with Z which is difficult to understand. This oscillatory variation with Z is also present in their data (not tabulated) at 136°. It is not clear whether their large value for holmium is associated with their observation of the largest IRD effect with holmium.

It is hoped that results of more detailed relativistic calculations and of experiments with extremely thin targets will be available in the future and that the outstanding deviations particularly in double-differential cross sections will then be understood. Further, attention is drawn once again to the challenging problem of reliable calculations of bremsstrahlung effects with relatively thick targets usually employed in such studies.

[1]G. Basavaraju, S. M. George, and P. P. Kane, Nucl. Instrum. Methods A **255**, 86 (1987).
[2]G. Basavaraju, P. P. Kane, and S. M. George, Phys. Rev. A **36**, 655 (1987).
[3]G. C. Spitale and S. D. Bloom, Phys. Rev. A **16**, 221 (1977).
[4]M. Gavrila, Phys. Rev. A **6**, 1348 (1972); **6**, 1360 (1972).
[5]V. Marchetti and C. Franck, Phys. Rev. A **39**, 647 (1989), and references mentioned therein.
[6]A. R. Reddy, K. Parthasaradhi, V. Laksminarayana, and S. Jnanananda, Proc. Phys. Soc. London **91**, 71 (1967).
[7]L. Pages, E. Bertel, H. Joffre, and L. Sklauenitis, At. Data **4**, 1 (1972).
[8]H. K. Tseng, R. H. Pratt, S. Yu, and Akiva Ron, Phys. Rev. A **17**, 1061 (1978).
[9]R. H. Pratt, H. K. Tseng, C. M. Lee, L. Kissel, C. MacCallum, and M. Riley, At. Data Nucl. Data Tables **20**, 175 (1977).
[10]R. K. Batra and M. L. Sehgal, Phys. Rev. B **23**, 4448 (1981).
[11]J. F. Perkins, Phys. Rev. **126**, 1781 (1962).
[12]H. A. Kramers, Philos. Mag. **46**, 836 (1923).
[13]W. W. Buechner, R. J. Van de Graaff, A. Sperduto, E. A. Buril, Jr., and H. Feshbach, Phys. Rev. **72**, 678 (1947).
[14]R. D. Evans, *The Atomic Nucleus* (McGraw-Hill, New York, 1955), Chap. 21.
[15]F. Schnaidt, Ann. Phys. (Leipzig) **21**, 89 (1934).
[16]Y. B. Bannett, D. L. Rapaport, and I. Freund, Phys. Rev. A **17**, 2011 (1977).
[17]L. A. Wittwer, Lawrence Livermore Laboratory Report No. UCRL-51268, 1972 (unpublished).
[18]I. B. Whittingham, Aust. J. Phys. **34**, 163 (1981).